NASA TM X-710

TECHNICAL MEMORANDUM

X-710

LONGITUDINAL AND LATERAL AERODYNAMIC CHARACTERISTICS AT MACH NUMBERS FROM 0.60 TO 2.20 OF A VARIABLE-SWEEP FIGHTER MODEL WITH WING SWEEP ANGLES FROM 25° TO 75°

By M. Leroy Spearman

Langley Research Center
Langley Station, Hampton, Va.

NATIONAL AERONAUTICS AND SPACE ADMINISTRATION
WASHINGTON August 1962

NATIONAL AERONAUTICS AND SPACE ADMINISTRATION

TECHNICAL MEMORANDUM X-710

LONGITUDINAL AND LATERAL AERODYNAMIC CHARACTERISTICS AT MACH NUMBERS FROM 0.60 TO 2.20 OF A VARIABLE-SWEEP FIGHTER MODEL WITH WING SWEEP ANGLES FROM 25° to 75°*

By M. Leroy Spearman

SUMMARY

An investigation has been made in the Langley 8-foot transonic pressure tunnel and the Langley 4- by 4-foot supersonic pressure tunnel at Mach numbers from 0.60 to 2.20 to determine the aerodynamic characteristics of a variable-sweep fighter model with wing sweeps varying from 25° to 75°.

The results of the investigation serve to illustrate the effectiveness of variable wing sweep in providing high subsonic lift-drag ratios together with low transonic drag rise and low supersonic wave drag. Although an aerodynamic-center shift of about 20 percent was obtained with varying sweep and Mach number, it is obvious that this variation can be controlled by a number of factors.

The directional stability characteristics were relatively unaffected by wing sweep and indicated a progressive decrease in directional stability with increasing angle of attack throughout the Mach number range. The effective dihedral for various wing sweeps varied erratically with angle of attack in the subsonic speed range although the variations were generally less for the highest wing sweep.

INTRODUCTION

The National Aeronautics and Space Administration is currently conducting studies directed toward the development of multimission fighter

*Title, Unclassified.

airplanes wherein variable wing sweep is employed as a means of combining efficient subsonic and supersonic flight characteristics. Various configurations have been included in these studies, and the results of some of the investigations are summarized in reference 1. The previous studies have included a wide variety of configurations in various speed regimes, and hence are not readily adaptable to systematic analysis. It is the purpose of this paper to present a summary of the results of an investigation conducted in a Mach number range from 0.60 to 2.20 on one configuration for which the wing sweep angle was varied progressively from 25° to 75°.

SYMBOLS

The results are referred to the stability-axis system with the exception of the lateral stability parameters which are referred to the body-axis system. The moment center is on the body center line at a point corresponding to the wing pivot location. All coefficients are based on the geometry of the 75° wing configuration which had a reference area of 1.212 square feet, a reference chord of 0.9 foot, and a reference span of 1.515 feet.

C_{L_α} lift-curve slope

$(L/D)_{max}$ maximum lift-drag ratio

$C_{D,o}$ drag coefficient at zero lift

$\frac{\Delta C_D}{C_L^2}$ drag-due-to-lift parameter

$C_{m,o}$ pitching-moment coefficient at zero lift

$\frac{\partial C_m}{\partial C_L}$ longitudinal stability parameter

$\frac{\partial C_m}{\partial i_t}$ horizontal-tail pitch effectiveness

C_{n_β} directional-stability parameter

C_{l_β}	effective-dihedral parameter
C_{Y_β}	side-force parameter
M	Mach number
Λ	sweep angle of leading edge of movable wing panel
α	angle of attack, deg
b	wing span
S	wing area
A	aspect ratio

MODEL AND APPARATUS

Details of the model are shown in figure 1. The outer wing panels could be rotated about the pivot point and sweep angles of 25°, 35°, 45°, 55°, 65°, and 75° were tested. The geometry for the various wing sweeps is tabulated in figure 1(b). The horizontal-tail incidence angle could be set at 0°, -5°, or -10° and both the horizontal and the vertical tails could be removed. The model was mounted on a six-component internal strain-gage balance.

TEST CONDITIONS

The model was tested in the Langley 8-foot transonic pressure tunnel at Mach numbers from 0.60 to 1.20 and in the Langley 4- by 4-foot supersonic pressure tunnel at Mach numbers of 1.41 and 2.20. The tests at transonic speeds were made at a stagnation pressure of 2,120 lb/sq ft with the Reynolds number per foot varying from 2,830,000 at M = 0.60 to 3,770,000 at M = 1.20. The tests at supersonic speeds were made at a stagnation pressure of 1,440 lb/sq ft with the Reynolds number per foot varying from 3,050,000 at M = 1.41 to 2,300,000 at M = 2.20. Transition strips of carborundum particles were applied near the nose and near the leading edges of the wing and tail surfaces in order to provide a turbulent boundary layer.

PRESENTATION OF RESULTS

The results of the investigation are presented in the following figures:

DISCUSSION

Longitudinal Characteristics

The variations of C_{L_α} with Mach number for various wing sweeps (fig. 2) indicate the generally expected reduction in Mach number effect as the wing sweep is increased. This feature, of course, provides the ability to reduce gust loads or buffet effects under some flight conditions. The effects of wing sweep on C_{L_α} are quite pronounced through the transonic speed range but in the supersonic speed range these effects rapidly diminish (fig. 3).

The characteristic drag rise is apparent in the transonic range for all wing sweeps (fig. 4). However, the drag rise is reduced and the Mach number at which the drag rise begins is increased as the wing sweep angle increases. Although sweep angle has only a slight effect on the subsonic drag level, the supersonic drag level decreases considerably with increasing sweep as the wave drag is reduced (figs. 4 and 5).

The variations of $(L/D)_{max}$ with Mach number (fig. 4) indicate one of the primary advantages of variable wing sweep in that relatively high values of lift-drag ratios can be obtained for subsonic cruise with aircraft that also have good transonic and supersonic flight potential. The effects of wing sweep angle on $(L/D)_{max}$ (fig. 5) indicate that at the lower Mach numbers still higher values of $(L/D)_{max}$ should be obtainable with sweep angles less than 25°. As the Mach number is increased, however, peak values of $(L/D)_{max}$ are obtained at progressively higher sweep angles because of the decrease in sweep effect on C_{L_α} and the increase in sweep effect on $C_{D,o}$. The drag-due-to-lift characteristics (figs. 6 and 7) indicate the trends with Mach number and wing sweep that would generally be expected on the basis of the lift-curve-slope variations.

The variation of longitudinal stability $\partial C_m/\partial C_L$ with Mach number (fig. 8) indicates characteristics that are generally typical of conventional tail-rearward designs. With fixed wing sweep, the aerodynamic center shifts rearward about 10 percent for the tail-off configuration and about 15 percent for the tail-on configuration. Because of an additional shift in aerodynamic center with wing sweep, the total rearward shift in aerodynamic center when operating as a variable-sweep aircraft with $\Lambda = 25°$ at subsonic speeds and $\Lambda = 75°$ at supersonic speeds is about 20 percent. The variations of $\partial C_m/\partial C_L$ with wing sweep (fig. 9) indicate an initial increase in stability as the wing panel is swept back to about 60° and then the stability level decreases with further increase in sweep. It is obvious that the variation of stability with wing sweep is quite sensitive and can be controlled by a number of factors such as pivot location, moment center, and area and planform of both the movable and the fixed portions of the wing.

The configuration displays positive values of $C_{m,o}$ throughout the Mach number range that are essentially unaffected by wing sweep (fig. 10). These positive values of $C_{m,o}$ are desirable, particularly at supersonic speeds, from the standpoint of reducing the trimming requirements and the drag due to trimming. The pitch effectiveness of the horizontal tail $\partial C_m/\partial i_t$ is essentially unaffected by wing sweep and indicates a variation with Mach number that would be expected on the basis of the tail lift-curve-slope variation (fig. 10).

Lateral Characteristics

The variations of sideslip derivatives with Mach number near zero angle of attack for the 75° wing sweep arrangement (fig. 11) are typical

of those for the other sweep arrangements and indicate results that are generally expected for conventional designs. The tail-off values of C_{Y_β} and C_{n_β} are nearly constant with Mach number whereas the tail-on values reflect the usual variation of vertical-tail lift-curve slope with Mach number. The tail-off values of C_{l_β} indicate a noticeable decrease from subsonic to supersonic speeds as the variation of wing lift-curve slope with Mach number reverses. An increase in tail contribution to C_{l_β} is indicated at supersonic speeds, apparently as a result of an outboard shift in tail center of pressure.

The variations of C_{n_β} with α for various wing sweeps (fig. 12) indicate little effect of sweep other than a slight increase in directional stability with increasing sweep at high angles of attack in the subsonic speed range. The directional stability progressively decreases with increasing angle of attack at each Mach number, and the indications are that directional instability would occur near $\alpha = 16^\circ$ throughout the Mach number range.

The variations of C_{l_β} with α for various wing sweeps (fig. 13) indicate rather erratic changes in the subsonic speed range. In general, the variations are less for the more highly swept wing because of the lower lift-curve slope for this wing. At supersonic speeds the variation of C_{l_β} with α is somewhat less than that at subsonic speeds.

CONCLUDING REMARKS

An investigation has been made in the Langley 8-foot transonic pressure tunnel and the Langley 4- by 4-foot supersonic pressure tunnel at Mach numbers from 0.60 to 2.20 to determine the aerodynamic characteristics of a variable-sweep fighter model with wing sweeps varying from 25° to 75°.

The results of the investigation serve to illustrate the effectiveness of variable wing sweep in providing high subsonic lift-drag ratios together with low transonic drag rise and low supersonic wave drag. Although an aerodynamic-center shift of about 20 percent was obtained with varying sweep and Mach number, it is obvious that this variation can be controlled by a number of factors.

The directional stability characteristics were relatively unaffected by wing sweep and indicated a progressive decrease in directional stability with increasing angle of attack throughout the Mach number range.

The effective dihedral for various wing sweeps varied erratically with angle of attack in the subsonic speed range although the variations were generally less for the highest wing sweep.

Langley Research Center,
National Aeronautics and Space Administration,
Langley Station, Hampton, Va., June 15, 1962.

REFERENCE

1. Polhamus, Edward C., and Hammond, Alexander D.: Aerodynamic Research Relative to Variable-Sweep Multimission Aircraft. Compilation of Papers Summarizing Some Recent NASA Research on Manned Military Aircraft. NASA TM X-420, 1960, pp. 13-38.

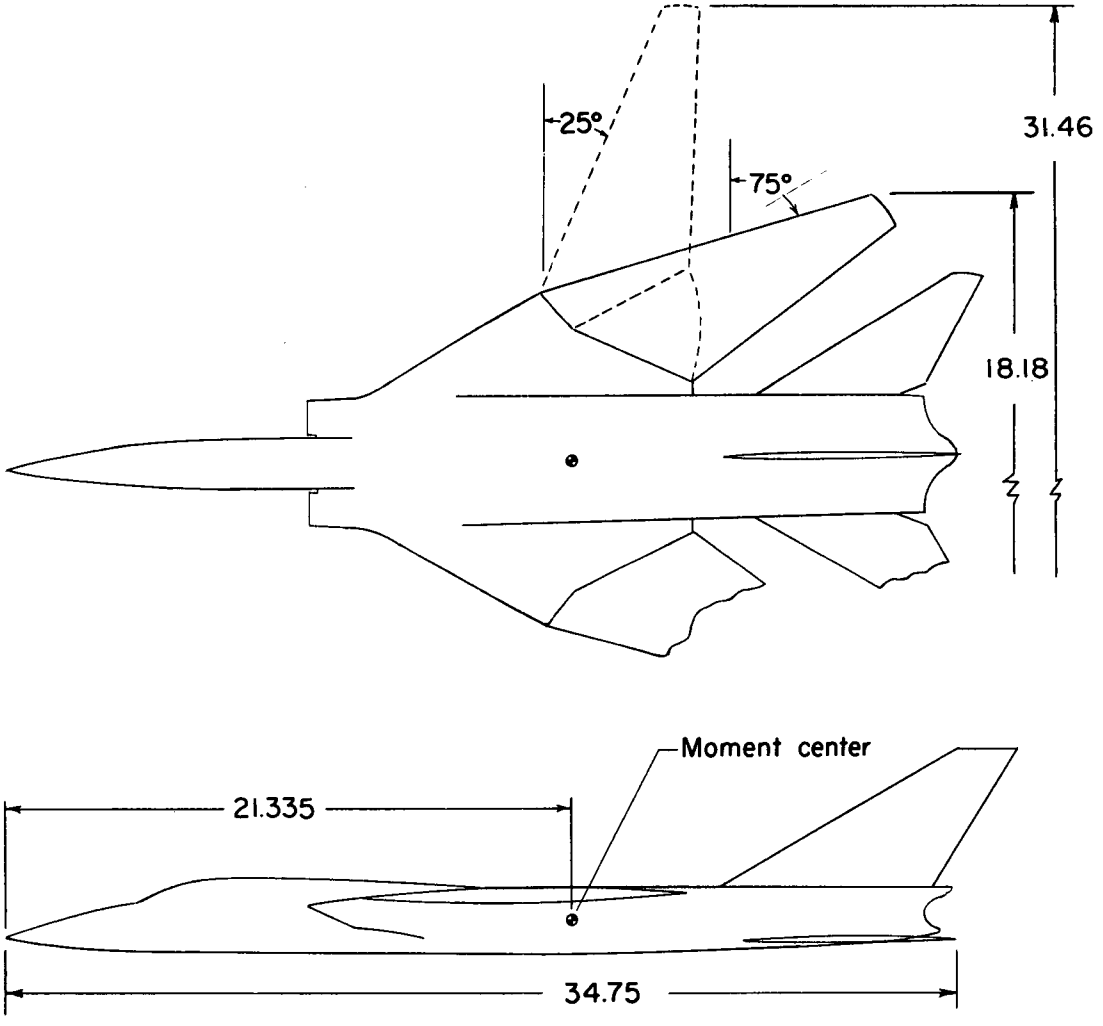

(a) General arrangement.

Figure 1.- Details of model. Dimensions in inches unless otherwise indicated.

Λ, deg	b, in.	S, sq in.	A
25	31.46	192.42	5.15
35	29.94	188.76	4.75
45	27.76	184.96	4.16
55	25.00	181.66	3.44
65	21.80	178.24	2.66
75	18.18	175.04	1.88

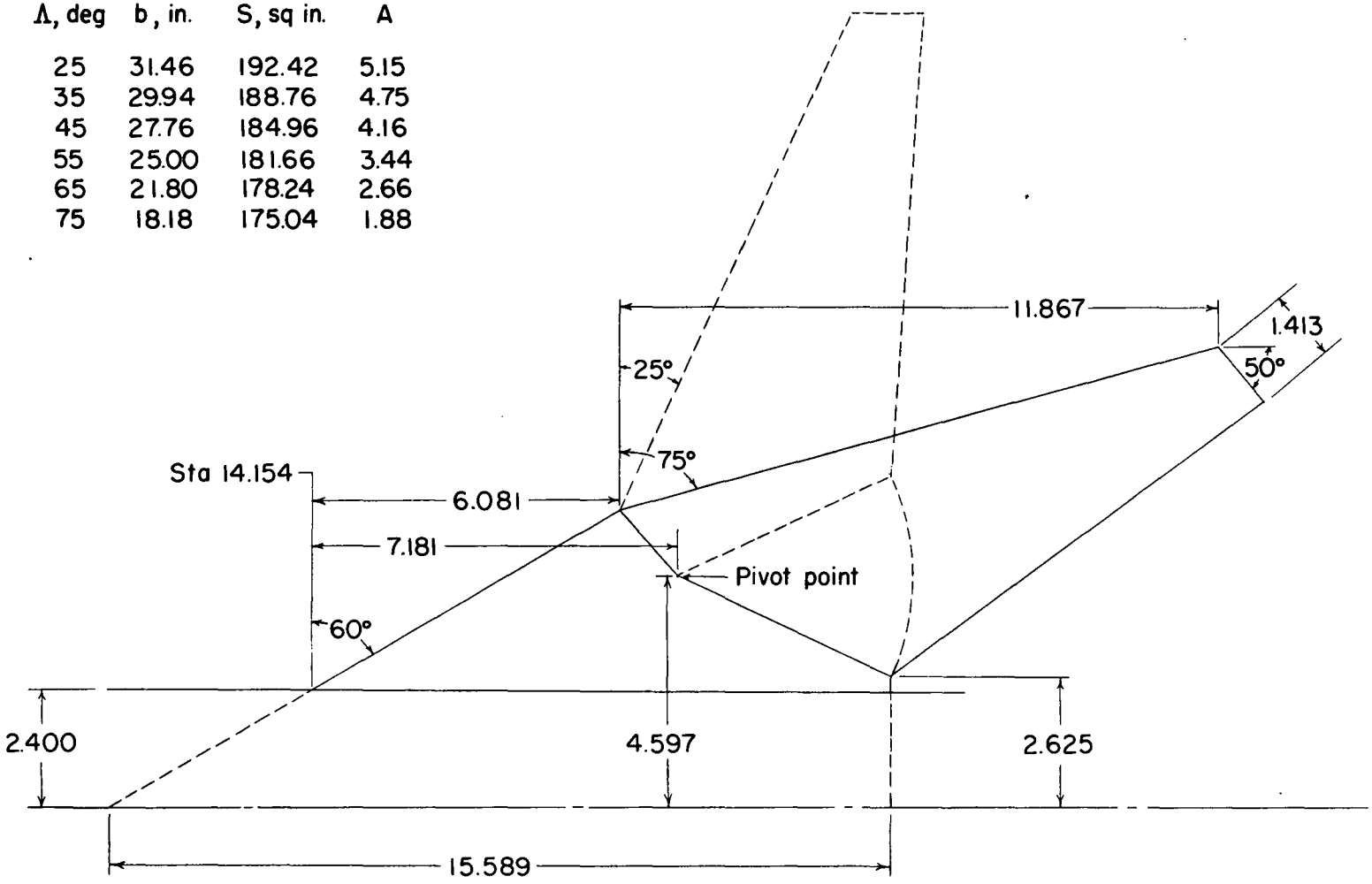

(b) Details of wing.

Figure 1.- Continued.

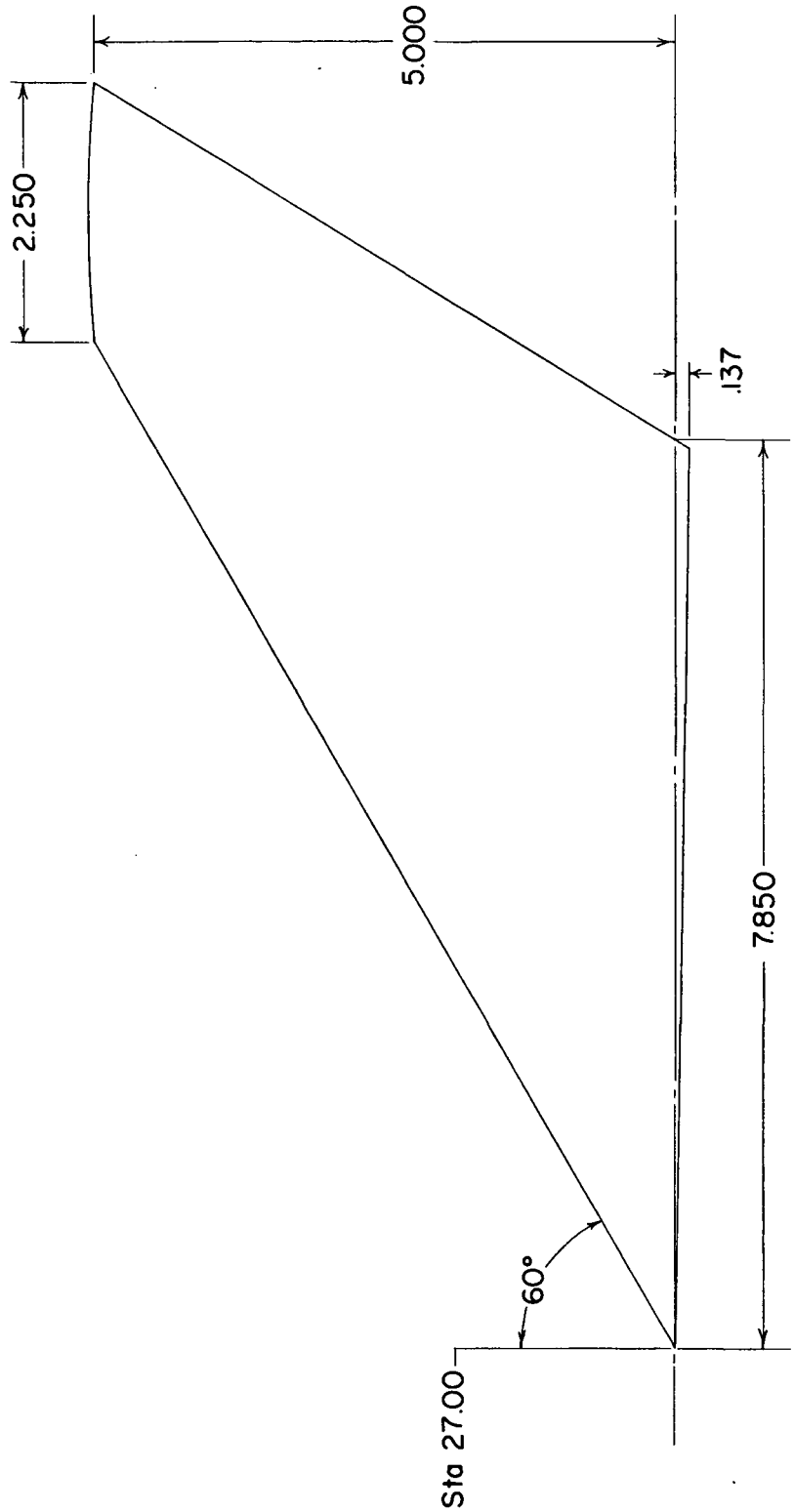

(c) Details of vertical tail.

Figure 1.- Continued.

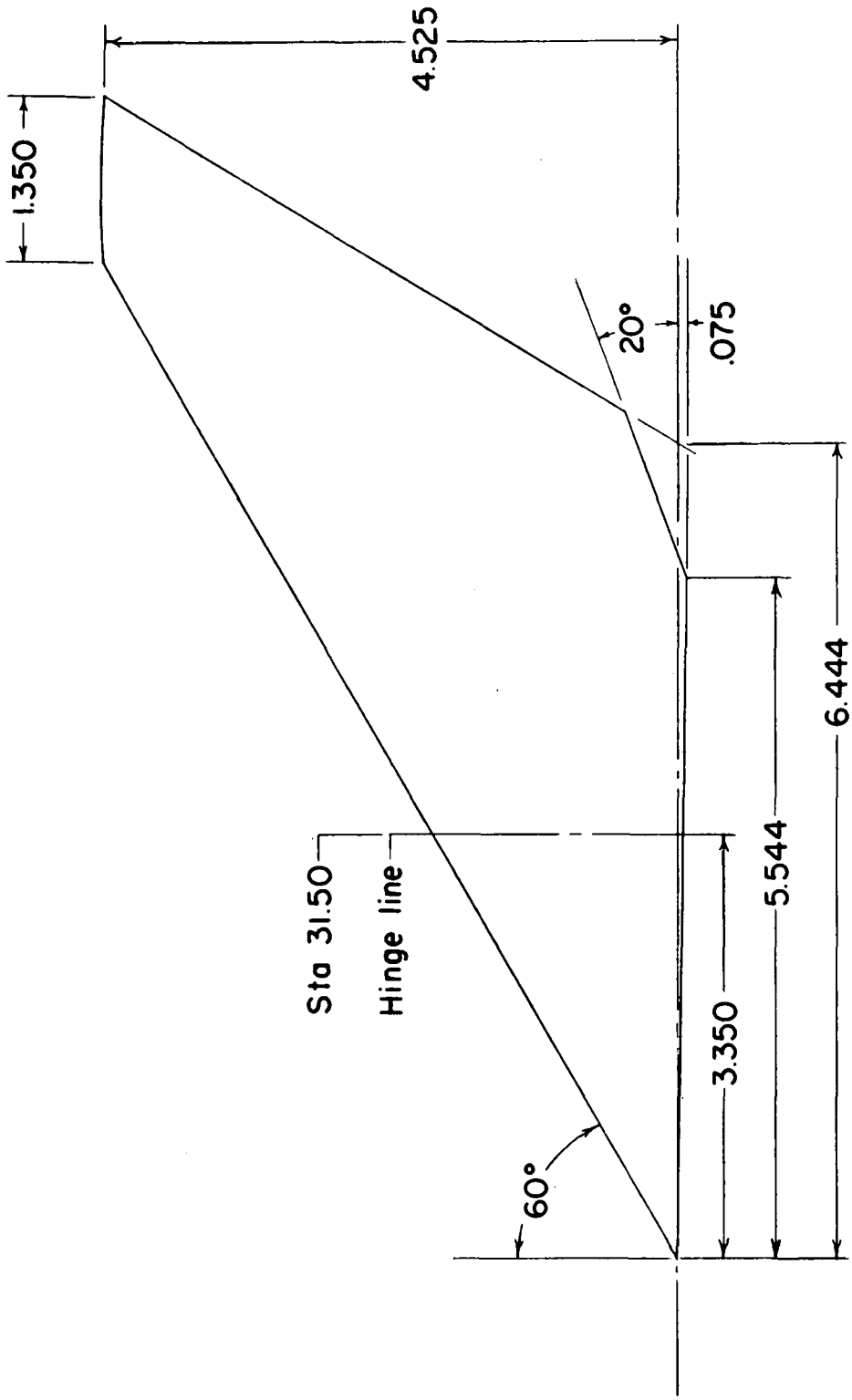

(d) Details of horizontal tail.

Figure 1.- Concluded.

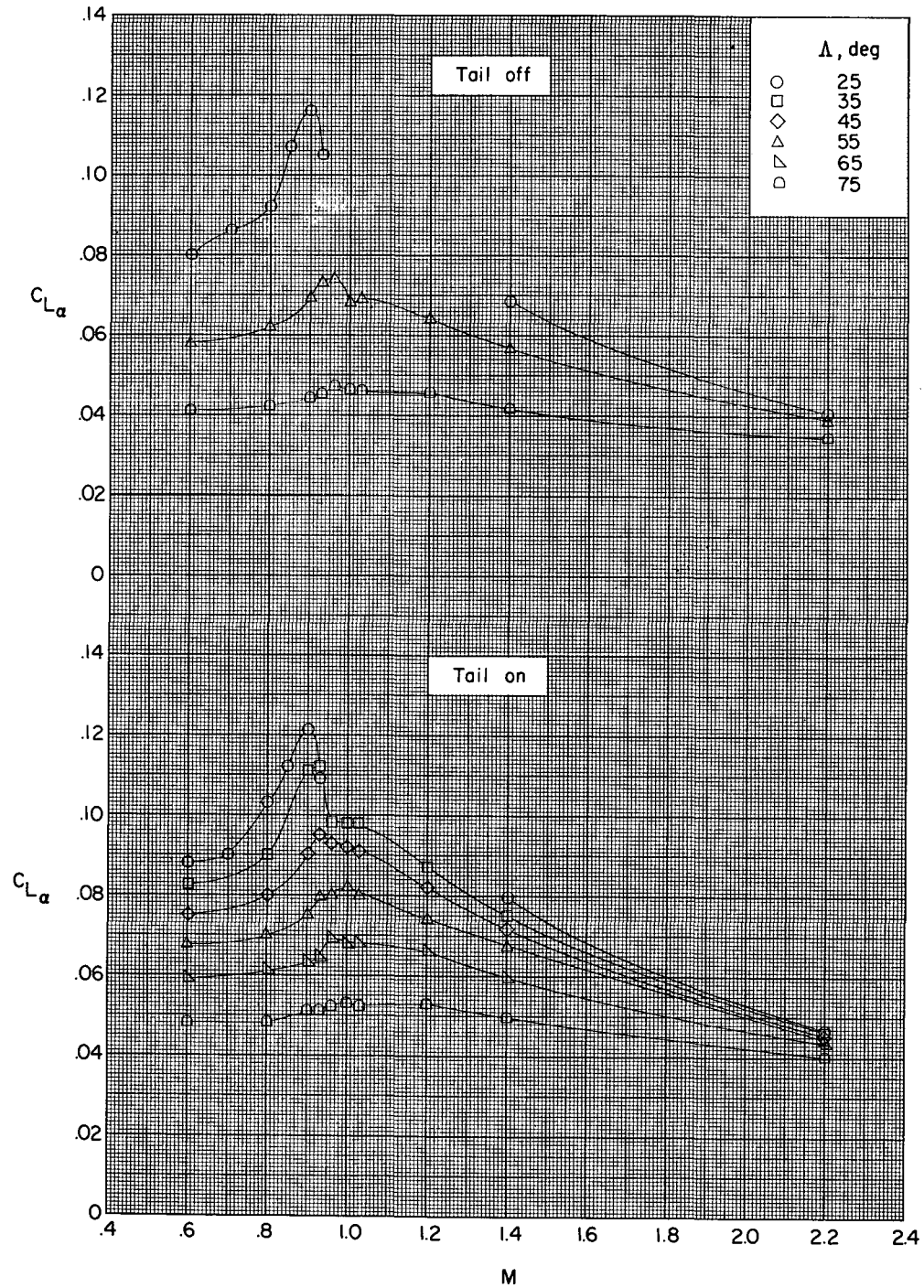

Figure 2.- Variation of C_{L_α} with Mach number for various wing sweep angles.

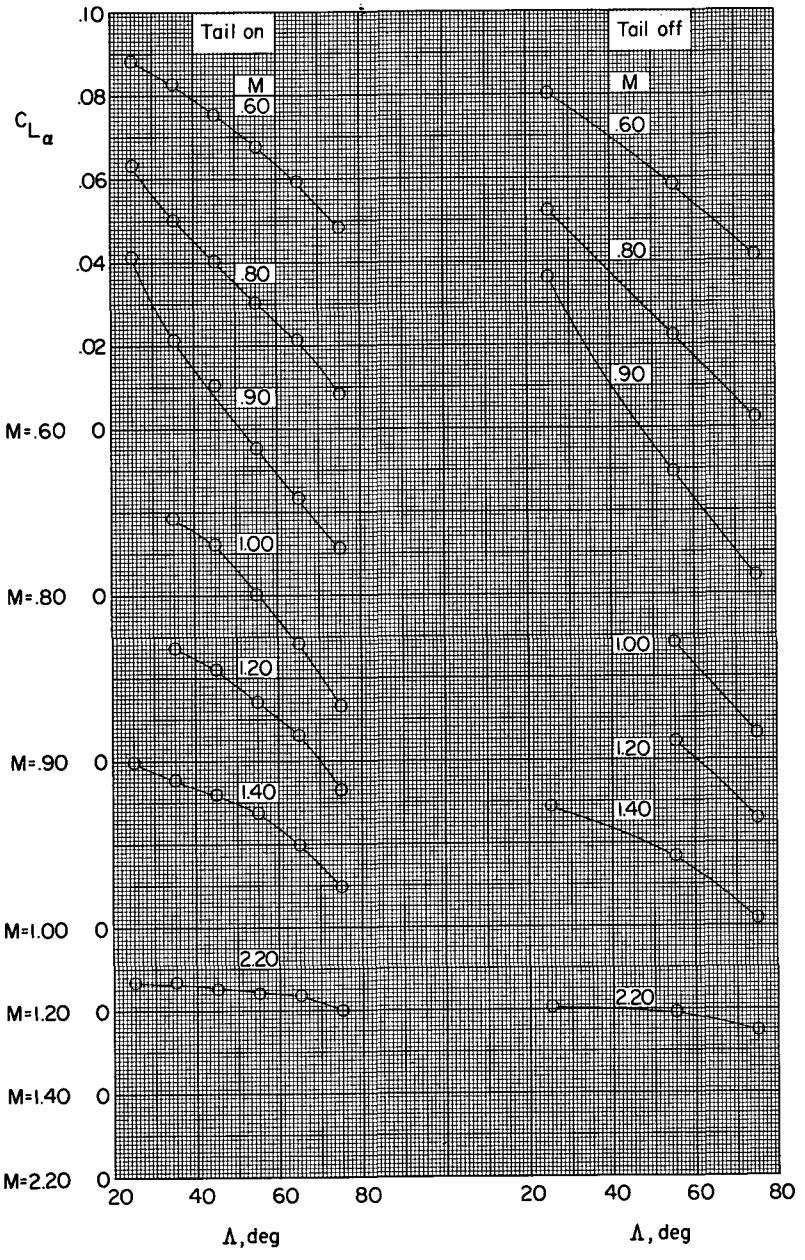

Figure 3.- Variation of C_{L_α} with wing sweep for various Mach numbers.

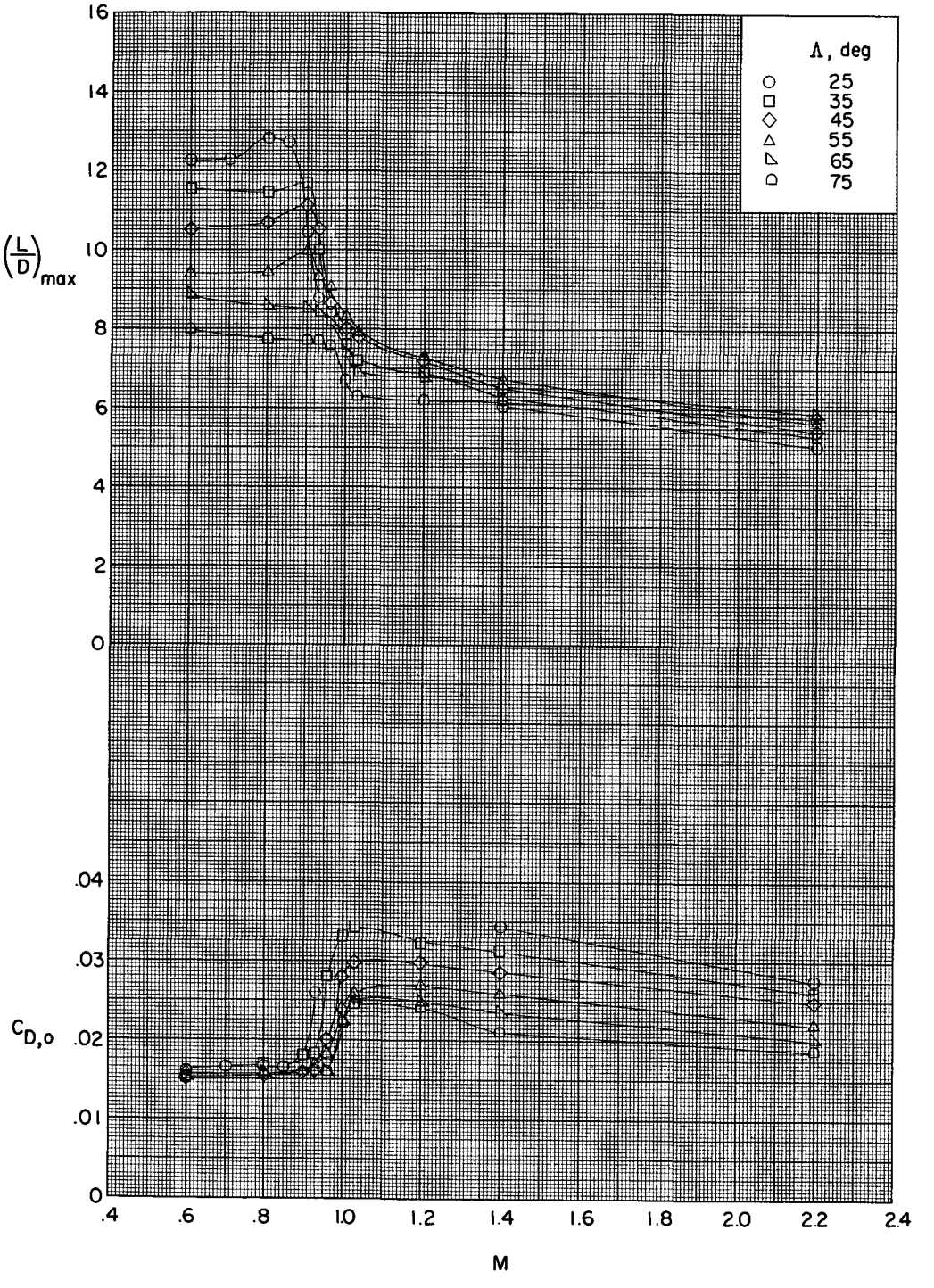

Figure 4.- Variation of $(L/D)_{max}$ and $C_{D,o}$ with Mach number for various wing sweep angles.

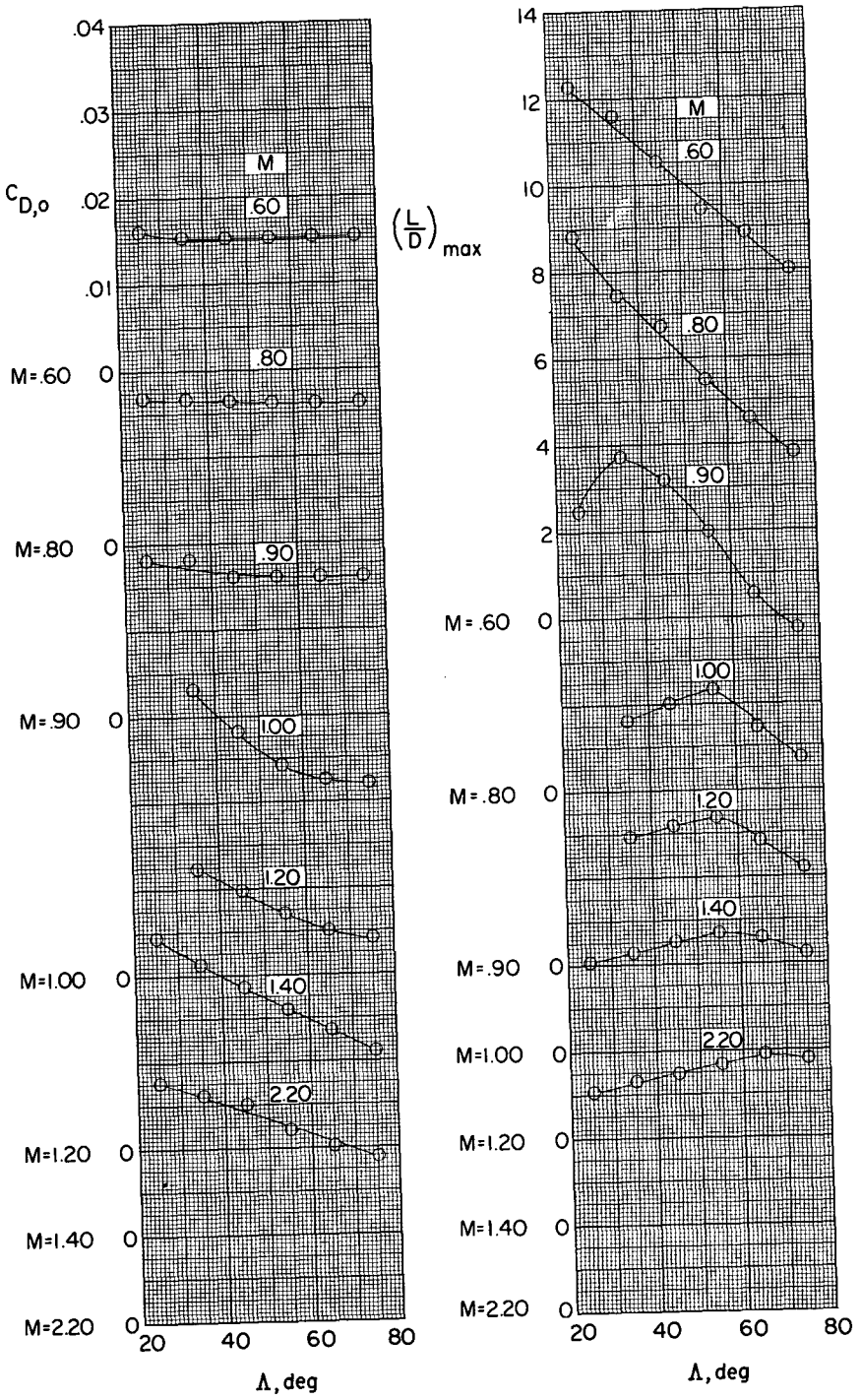

Figure 5.- Variation of $(L/D)_{max}$ and $C_{D,o}$ with wing sweep for various Mach numbers.

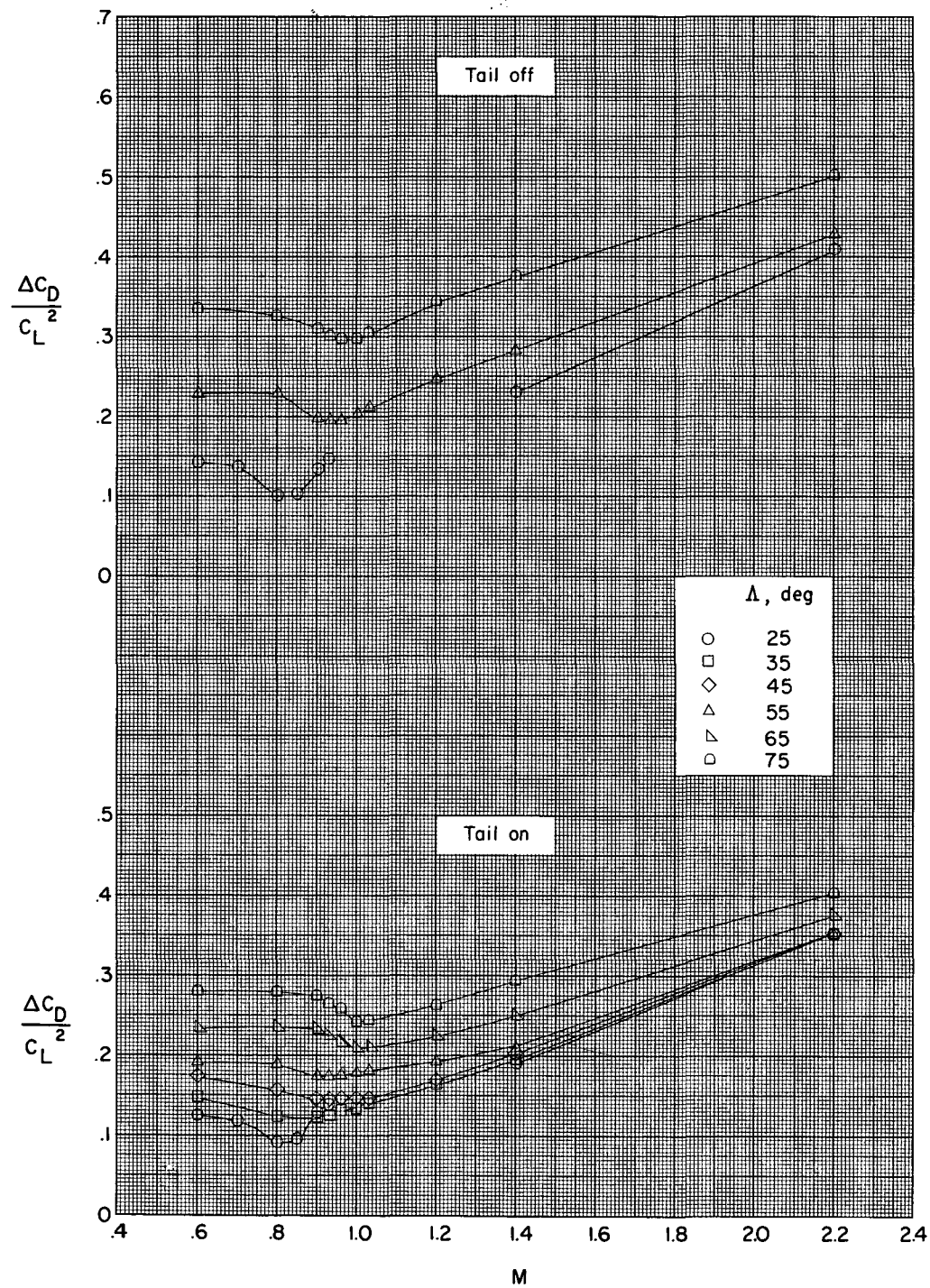

Figure 6.- Variation of $\frac{\Delta C_D}{C_L^2}$ with Mach number for various wing sweep angles.

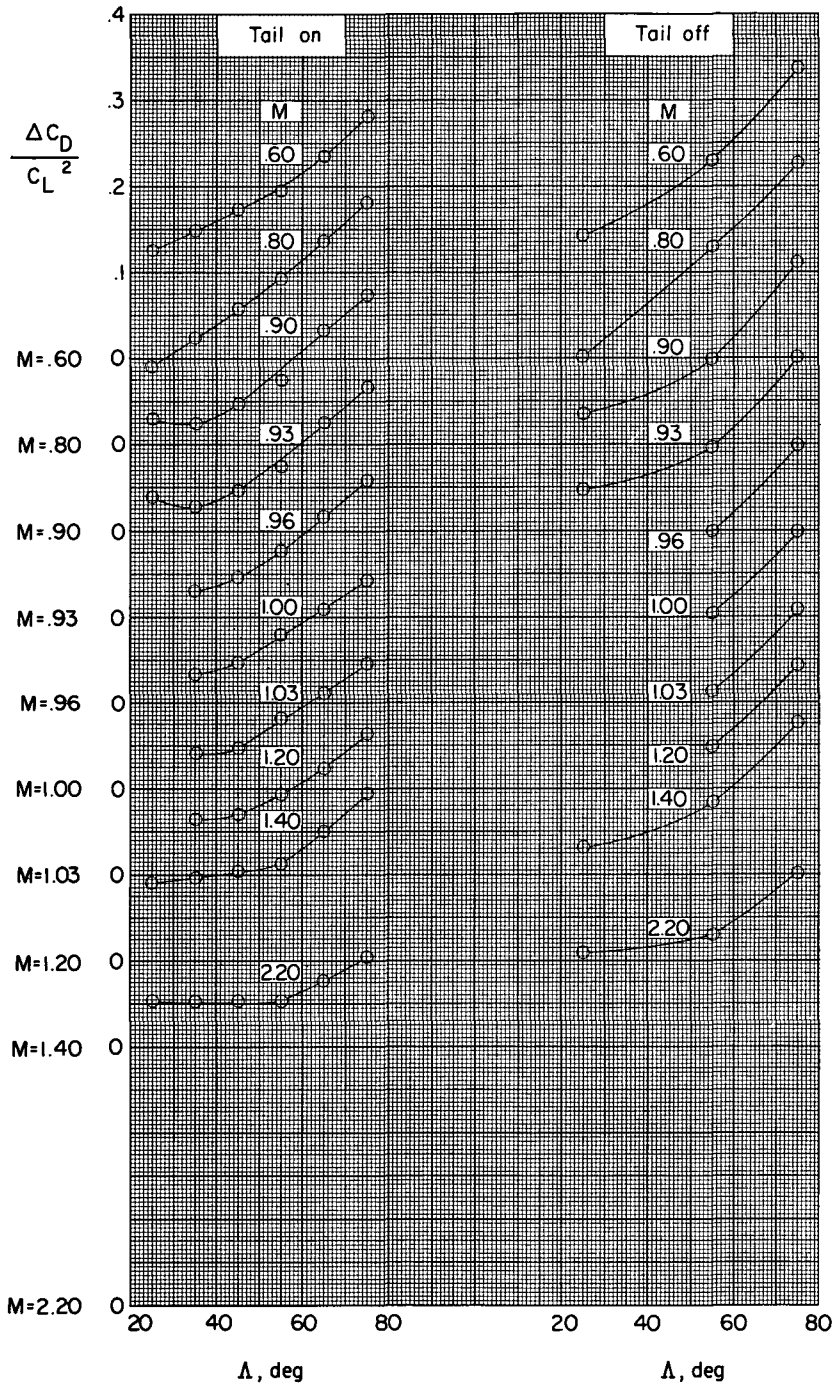

Figure 7.- Variation of $\frac{\Delta C_D}{C_L^2}$ with wing sweep for various Mach numbers.

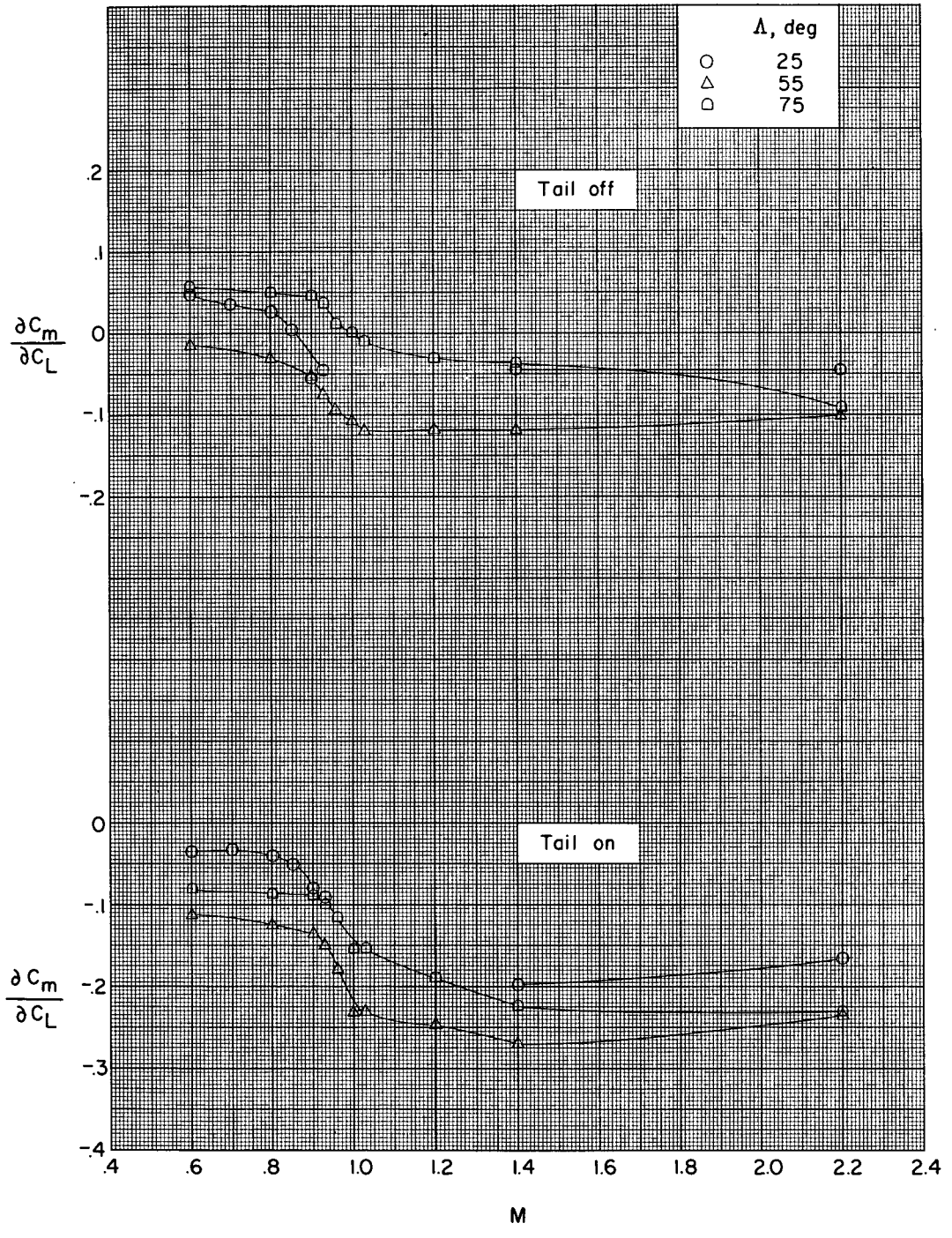

Figure 8.- Variation of $\frac{\partial C_m}{\partial C_L}$ with Mach number for various wing sweep angles.

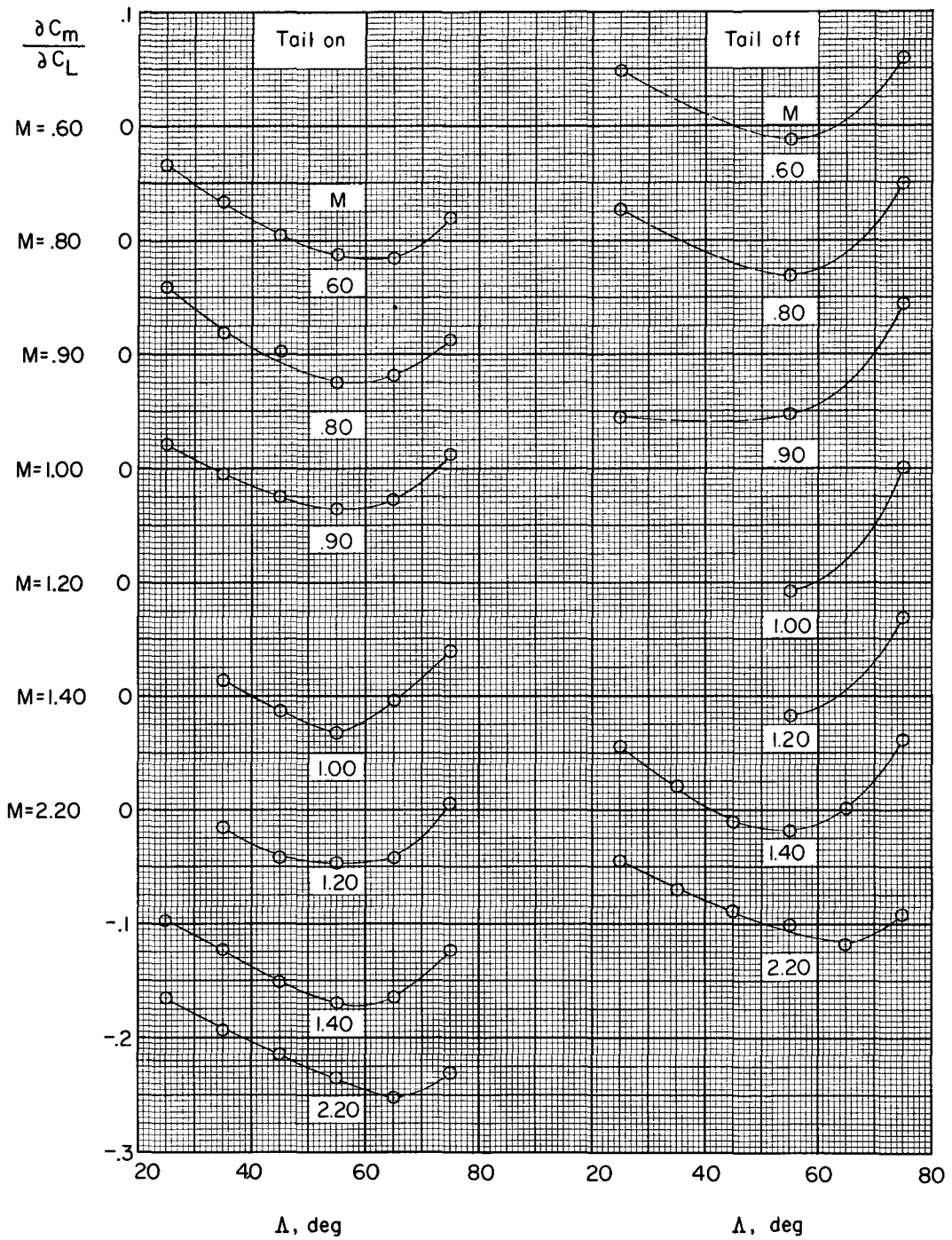

Figure 9.- Variation of $\frac{\partial C_m}{\partial C_L}$ with wing sweep for various Mach numbers.

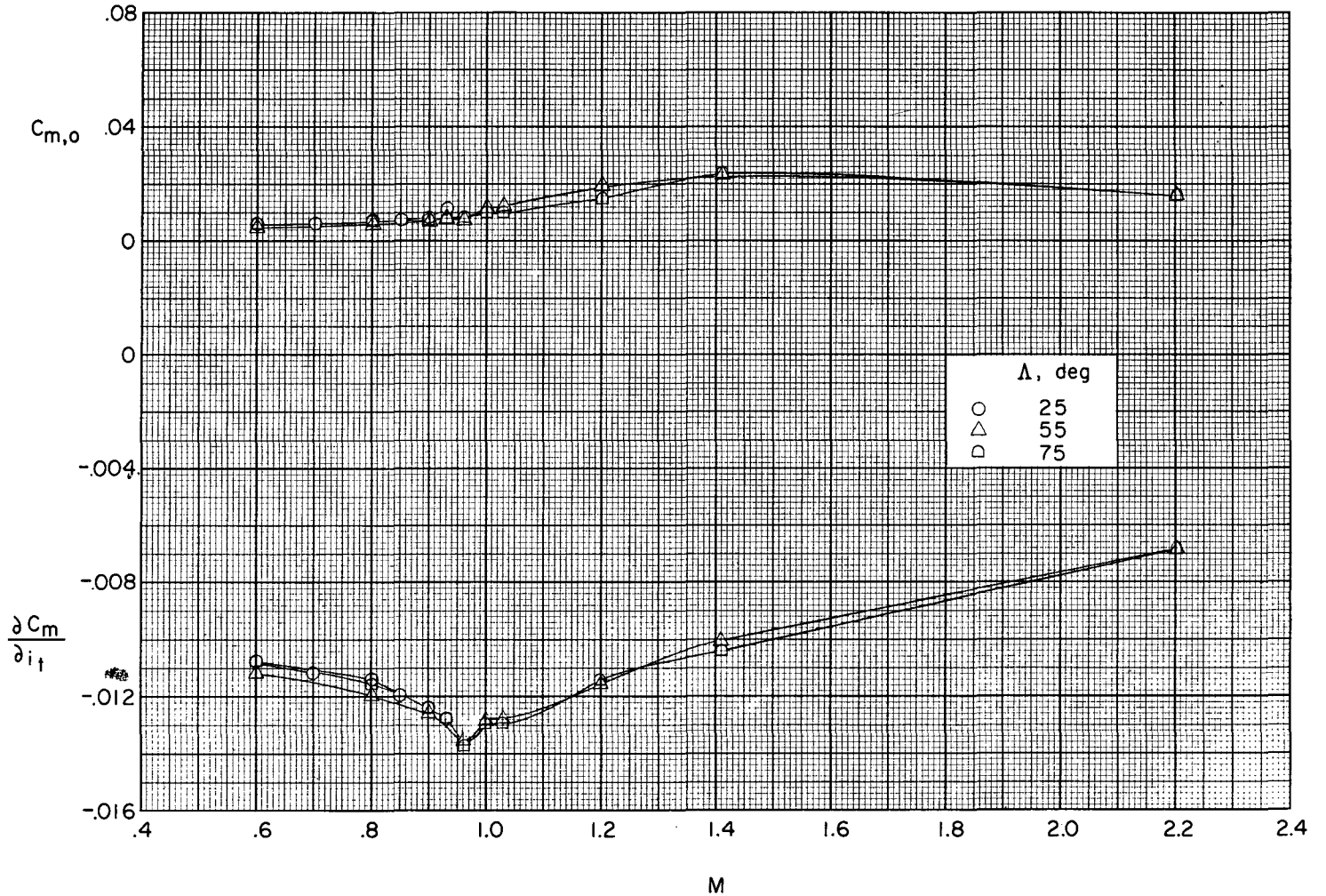

Figure 10.- Variation of $C_{m,o}$ and $\frac{\partial C_m}{\partial i_t}$ with Mach number for various wing sweep angles.

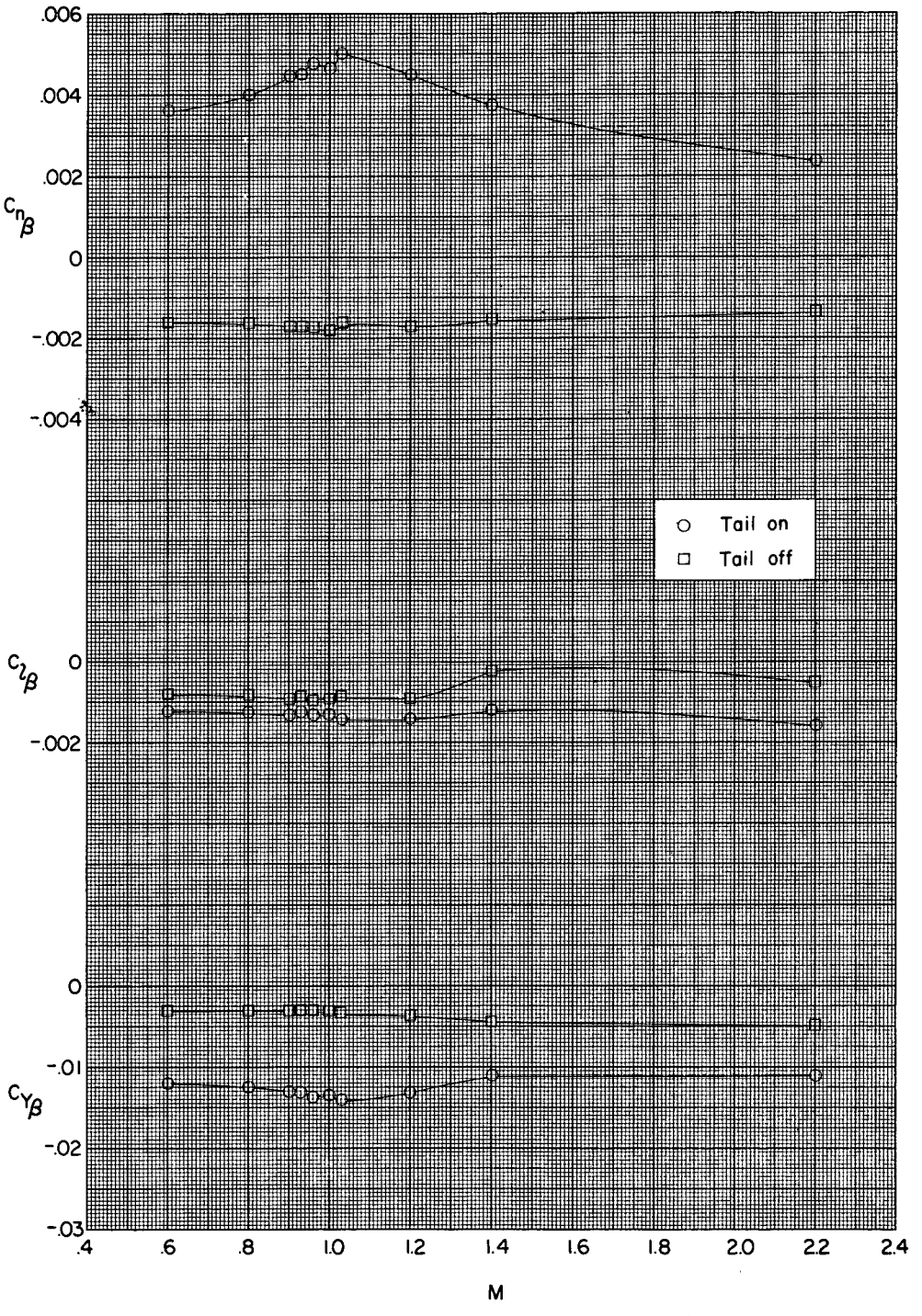

Figure 11.- Variation of sideslip derivatives with Mach number. $\Lambda = 75^{\circ}$; $\alpha \approx 0^{\circ}$.

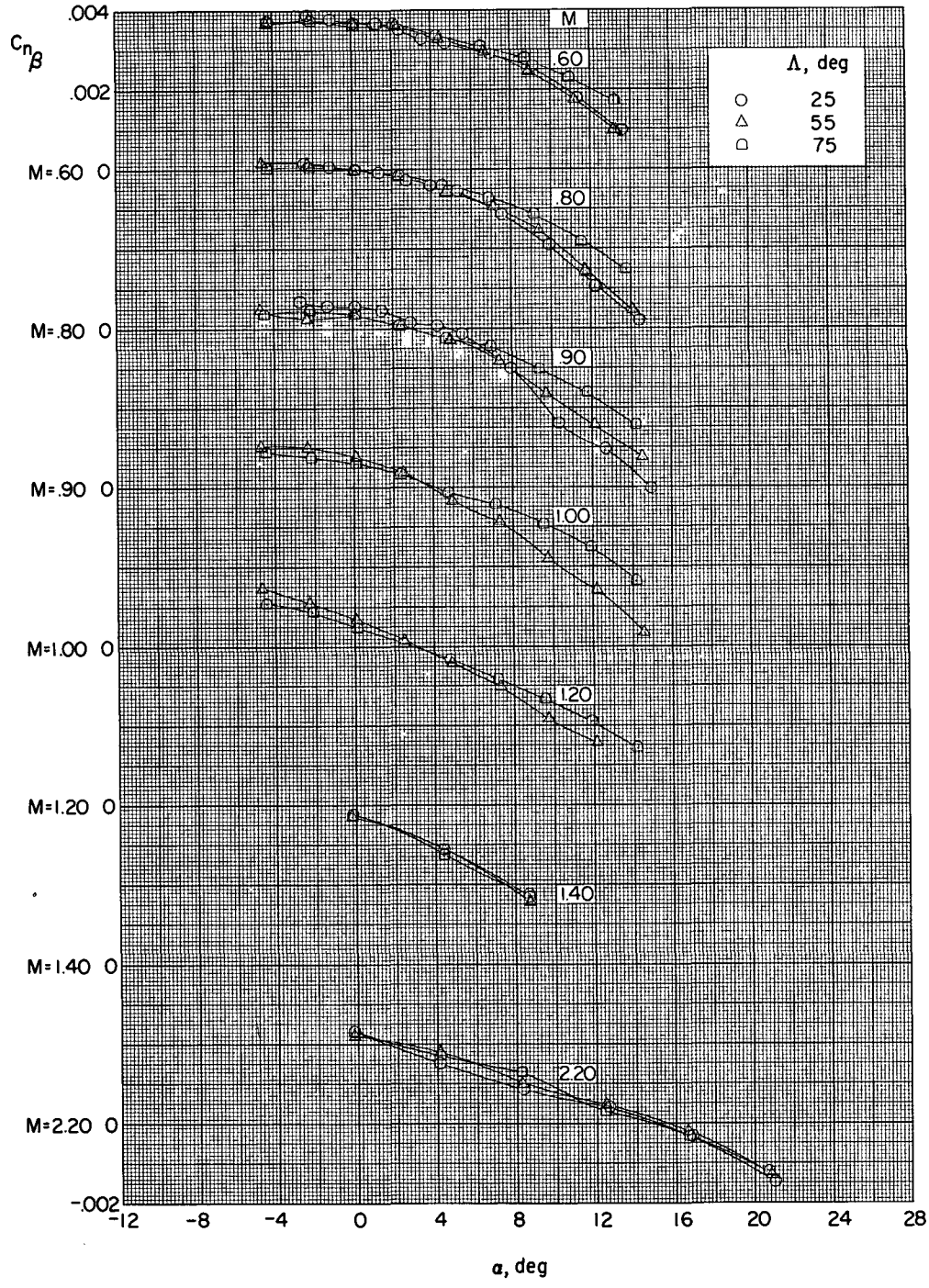

Figure 12.- Variation of C_{n_β} with angle of attack for various wing sweep angles. Tail on.

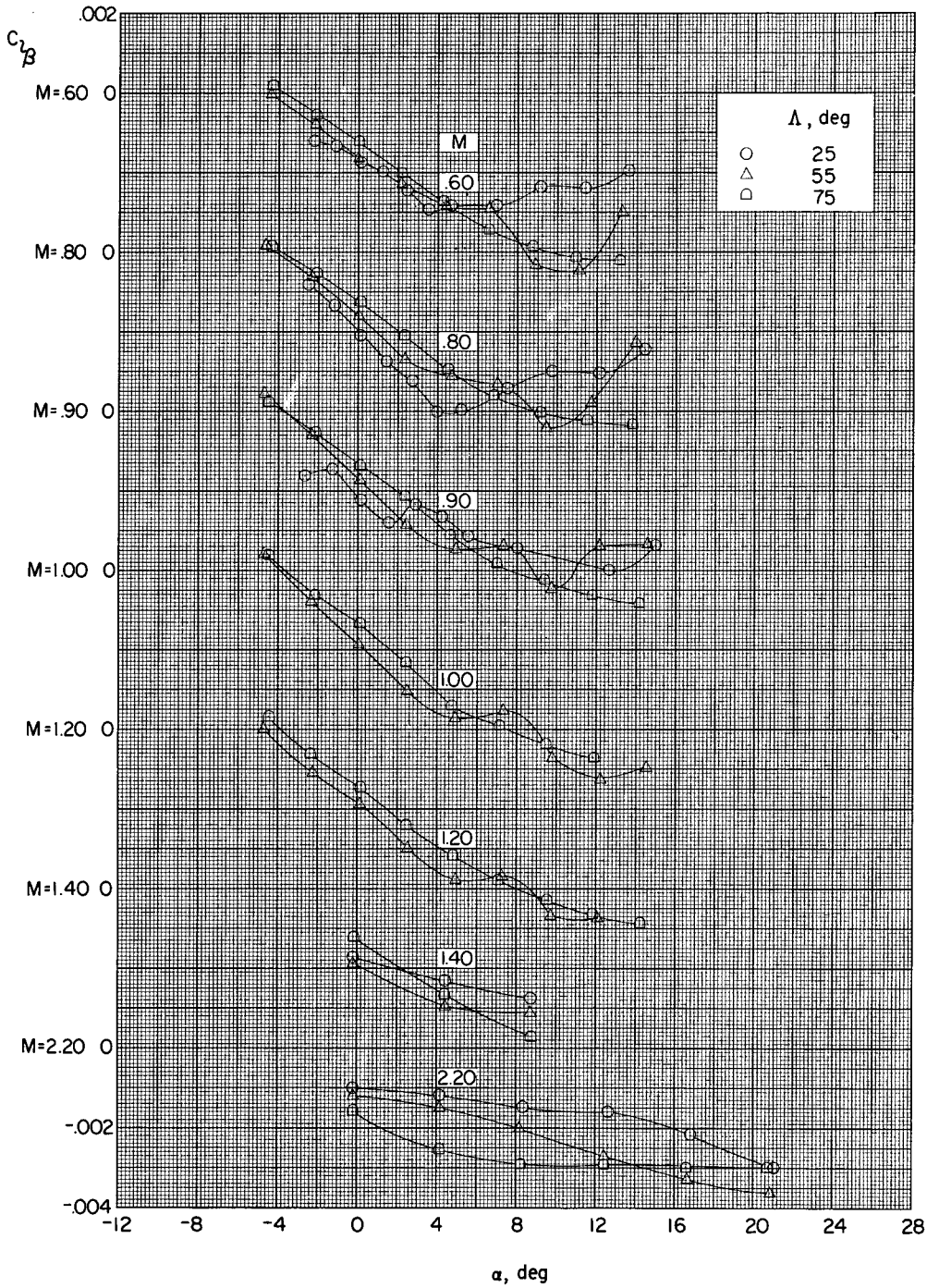

Figure 13.- Variation of C_{l_β} with angle of attack for various wing sweep angles. Tail on.